Charge Ordered States in $La_{1-x}Sr_xFeO_3$

J. Q. Li,[1,*] Y. Matsui,[1] S. K. Park,[2] and Y. Tokura[2]
[1]*National Institute for Research in Inorganic Materials, 1-1 Namiki, Tsukuba, Ibaraki 305, Japan*
[2]*Department of Applied Physics, University of Tokyo, Tokyo 113, Japan*
(Received 17 March 1997)

The presence of complex charge ordering (CO) phenomena in $La_{1-x}Sr_xFeO_3$ $(0 \le x \le 0.7)$ has been revealed by transmission electron microscopy at low temperatures. In $La_{0.7}Sr_{0.3}FeO_3$ $(x = 0.3)$ the precursory CO reflections become visible as streaks at ~250 K upon cooling. Below 150 K these streaks condense to sharp spots at the systemic $(\frac{1}{2}, 0, 0)$ positions. The real-space images are suggestive of charge segregation occurring at low temperatures. At high doping levels $(0.5 \le x \le 0.7)$, the CO has been observed in the $\langle 111 \rangle_p$ direction below ~200 K. In particular, the results obtained $La_{0.3}Sr_{0.7}FeO_3$ $(x = 0.7)$ can be well understood in terms of CO in sequence $\ldots Fe^{3+}Fe^{3+}Fe^{5+}Fe^{3+}Fe^{3+}Fe^{5+}\ldots$, as proposed previously. [S0031-9007(97)03543-6]

PACS numbers: 75.30.Kz, 64.70.Rh, 71.38.+i, 75.50.Cc

It has been known that charge carrier doping can induce extraordinary phenomena in transition metal oxides with perovskite-related structure, e.g., high T_c superconductivity [1], electronic phase separation [2], and charge ordering [3]. Recently, another remarkable behavior of doped charge carries, the colossal magnetoresistance, has been discovered in perovskite type manganites $L_{1-x}A_xMnO_3$ (L = rare earth, A = alkaline earth) [4,5]. It has also been found that certain fascinating features are related to charge and spin dynamics in this system [3]. In fact, the charge ordering (CO) and its magnetic-field-melting mechanism is one of the most important issues in the present studies for the colossal magnetoresistive manganites. For this reason, the study of closely related CO systems is extremely useful. The charge disproportionation and spin dynamics in $La_{1-x}A_xFeO_3$ (A = Sr and Ca) perovskite have been investigated in the past [6–8]. The charge disproportionation was first detected by Mössbauer spectroscopy at the temperature of about 4 K in the sample $La_{0.33}Sr_{0.67}FeO_3$ $(x = \frac{2}{3})$, in which two kinds of Fe ions with valence states +3 (Fe^{3+}) and +5 (Fe^{5+}) were found with the ratio ~2:1 [7]. The resistivity also shows a jumplike increase at the transition temperature (~207 K) with a narrow thermal hysteresis signaling the occurrence of first-order phase transition [8]. It is worth noting that the Fe^{5+} valence is unconventionally high, and which shows the full spin up occupancy of the t_{2g} state. Furthermore, such an anomalous valence state as well as real space ordering of valence-skipping sites was observed by the measurements of magnetic neutron scattering [6], which indicated that the ordered layers of Fe^{3+} and Fe^{5+} ions are in the sequences of ...335335.. along the $\langle 111 \rangle$ direction of the perovskite structure. However, the direct evidence of the structural changes accompanying the CO has not been obtained. In this paper, we report the results on electron diffraction and electron microscopy studies of $La_{1-x}Sr_xFeO_3$ $(0 \le x \le 0.7)$ at low temperatures. The electron diffraction evidences for presence of different kinds of CO phenomena at low and high doping levels are presented. The structural modulations related to the cooperative ordering of charges and spins in $La_{0.3}Sr_{0.7}FeO_3$ have been directly identified.

Single crystalline samples of the $La_{1-x}Sr_xFeO_3$ $(0 \le x \le 1)$ samples were melt grown by the floating-zone method; the detailed process of the sample preparation is described in Ref. [8]. Transport and magnetic susceptibility measurements indicated anomalies arising from the charge disproportionation for the samples with $0.65 \le x \le 0.7$, in which two kinds of Fe ions with valence states +3 (Fe^{3+}) and +5 (Fe^{5+}) were determined at low temperature. The resistivity shows a jumplike increase at about 207 K with a narrow thermal hysteresis [8]. For electron diffraction and high resolution electron microscopy studies, the samples were ground under CCl_4, dispersed on Cu grids coated with holy-carbon support files, and examined with a Hitachi H-1500 high resolution microscope operated at 800 kV. The crystal structure of the $La_{1-x}Sr_xFeO_3$ system at room temperature is that of a distorted perovskite; the structural distortion depends on the Sr doping level. The average structure of this system can be considered as a face-centered-cubic (fcc) structure with lattice parameter $a = 2a_p \approx 0.78$ nm over the range of composition $0.3 \le x \le 0.7$. However, for facilitating the comparisons of the CO phenomena, in this paper we keep the simple cubic perovskite cell notion.

The electron microscopy observations of the ordered states in $La_{1-x}Sr_xFeO_3$ $(0 \le x \le 0.7)$ at low temperatures show a wide variety of satellite reflections depending on x, indicating a rich variety of structural phenomena. First, we shall discuss the results obtained for $x = 0.3$; Figs. 1(a)–1(c) show a series of [001]-zone electron diffraction patterns obtained between 240 and 110 K on the same crystal grain. The main diffraction spots with high intensity are indexed with the perovskite structure. In addition to the main diffraction spots, the weak satellite reflections have been exhibited. Upon cooling from room temperature, these satellite reflections mostly become

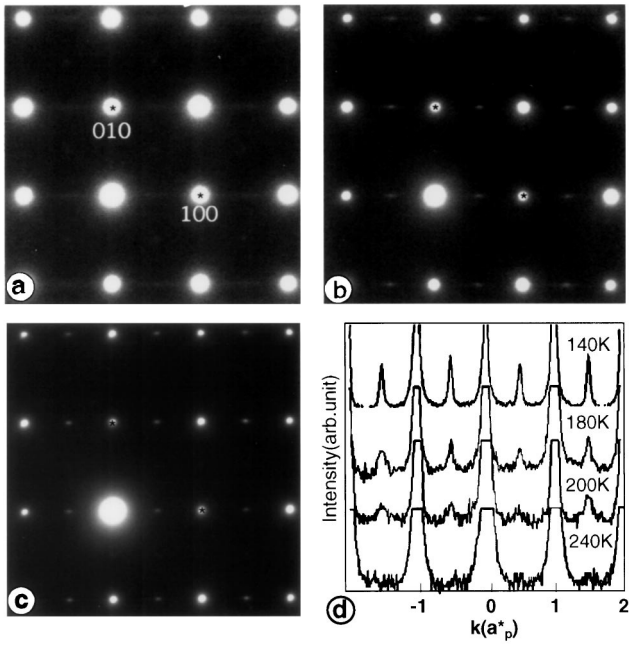

FIG. 1. [001] zone-axis electron diffraction patterns of $La_{0.7}Sr_{0.3}FeO_3$ obtained at (a) 240 K, (b) 180 K, and (c) 110 K, respectively. The presence and changes of superlattice reflections have been evident. (d) The microphotometric density curves along the [100] direction showing the temperature condensation of the superlattice reflections.

visible below ~250 K as the diffuse streaks, which are centered at the systematic $(\frac{1}{2}, 0, 0)$ positions and elongated along the $\langle 100 \rangle$ direction. These diffraction streaks contract progressively and slowly to their center positions, and below ~150 K they show up as superlattice spots. In Fig. 1(d) we show the microphotometric density curves along the $\langle 100 \rangle$ direction, exhibiting the changes of the intensity and width of superstructural peaks with varying temperature. The peak width decreases slowly as the temperature goes down. It was noticed, however, that the results obtained in our investigations could vary slightly from grain to grain. Weak diffraction streaks can be found occasionally even at room temperature in some crystals, which may be due to the inhomogeneous distribution of Sr dopants. Furthermore, as a common structural feature in the perovskite system [3], the twin domains rotated by 90° with respect to one another have been frequently observed in our investigations at low temperature; i.e., two perpendicular sets of satellite reflections around each main spot appear in the diffraction pattern. The size of the domains varies from a few hundred to several thousand angstroms. A similar structural phenomenon has also been observed in $La_{0.6}Sr_{0.4}FeO_3$ ($x = 0.4$), and in this case the superlattice reflections were observed just below ~220 K.

It seems to be impossible to correlate this kind of ordering phenomenon with the oxygen deficiency and other possible chemical inhomogeneities in the crystals. Though the issue of oxygen inhomogeneity can be rather complicated, from a chemical point of view it seems unrealistic that the oxygen deficiency alone can account for the superstructure with wave vector $\mathbf{Q} = a_p^*[\frac{1}{2}, 0, 0]$ in the nearly stoichiometeric sample of $La_{0.7}Sr_{0.3}FeO_3$ (where $a_p^* a_p = 2\pi$). Hence, we propose that the superstructural modulation observed in $La_{1-x}Sr_xFeO_3$ ($0.3 \leq x \leq 0.4$) originates from CO occurring at low temperature. In fact, the magnetic susceptibility measurements indicated some changes below ~150 K for $x = 0.3$ [8], which may be correlated with the CO transition we observed.

Valence states of the Fe in the $La_{1-x}Sr_xFeO_3$ system have been investigated by means of the Mössbauer spectroscopy previously [7,9]. At low temperature, a model based on charge disproportionation of Fe^{3+} and Fe^{5+} has been proposed for $x \sim \frac{2}{3}$ [6]. While in a lower Sr-doping range ($x \leq 0.4$), the experimental results showed that the valence states of Fe ions are +3 or +4, and Gallagher *et al.* stated to have observed the resolution into the distinct valence states of Fe^{3+} and Fe^{4+} at ~4 K [9]. Hence, we propose that the superstructural modulation observed in $x = 0.3$ is due to the ordering of Fe^{3+} and Fe^{4+} at low temperature. Furthermore, it has also been noted that in the $La_{0.7}Sr_{0.3}FeO_3$ crystal the Fe^{4+} and Fe^{3+} ions have a ratio of about 1:2; if the localized charges could have a uniform density (as is usually assumed) and adopt the ordering in the lattice similar to other related systems, e.g. (La,Ca)MnO_3 and $(La,Sr)_2NiO_4$ [3,10], the CO modulation should have the wave vector $\mathbf{Q}' = a_p^*[\frac{1}{3}, 0, 0]$ rather than $a_p^*[\frac{1}{2}, 0, 0]$ as we observed. In order to address this discrepancy, a series of high resolution images have been obtained between 110 K and room temperature. It is found that the observations can be well understood by charge segregation occurring at low temperature [2]. Figure 2(a) shows a typical high resolution image taken at ~140 K. Segregation of charges occurs to form the perfect charge ordered state of concentration $n_c = \frac{1}{2}$ in the charge rich areas. So there are almost as many Fe^{4+} ions as Fe^{3+} ions in the charge rich areas, and in the other Fe^{4+} poor areas, the Fe ions are almost Fe^{3+}. The average ratio of Fe^{3+} and Fe^{4+} could be given as 2:1. We show in Fig. 2(b) a schematic picture of ionic ordering of Fe^{4+} and Fe^{3+} corresponding to the CO wave vector $\mathbf{Q} = a_p^*(\frac{1}{2}, 0, 0)$, which only represents the ordered state in charge rich areas. It is clearly exhibited that the well-defined ordered state in Fig. 2(a) can be found only in some small areas. The coherence length of the ordered state at around 110 K is found to be about 5–10 nm along the *a*-axis direction. The high resolution images taken at low temperature always show complex variations of contrast. The detailed results about the microstructural properties of $La_{1-x}Sr_xFeO_3$ ($0 \leq x \leq 1$) will be reported in a separate paper [8].

We now focus on the investigation of CO in the samples with higher Sr doping. The electron diffraction at low temperatures exhibits the CO along the $\langle 111 \rangle_{\mathbf{p}}$ direction for $0.5 \leq x \leq 0.7$. Especially, very sharp

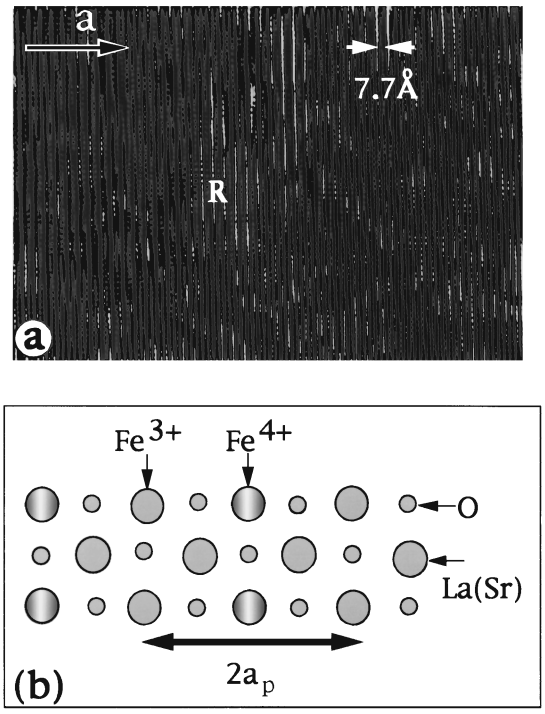

FIG. 2. (a) The typical high resolution image slightly off the [001] zone obtained at ~140 K exhibiting the domain structure caused by charge segregation in $La_{0.7}Sr_{0.3}FeO_3$. A hole rich area is indicated by *R*. (b) A schematic picture showing the possible CO state of Fe^{4+} and Fe^{3+} ions in the charge rich areas.

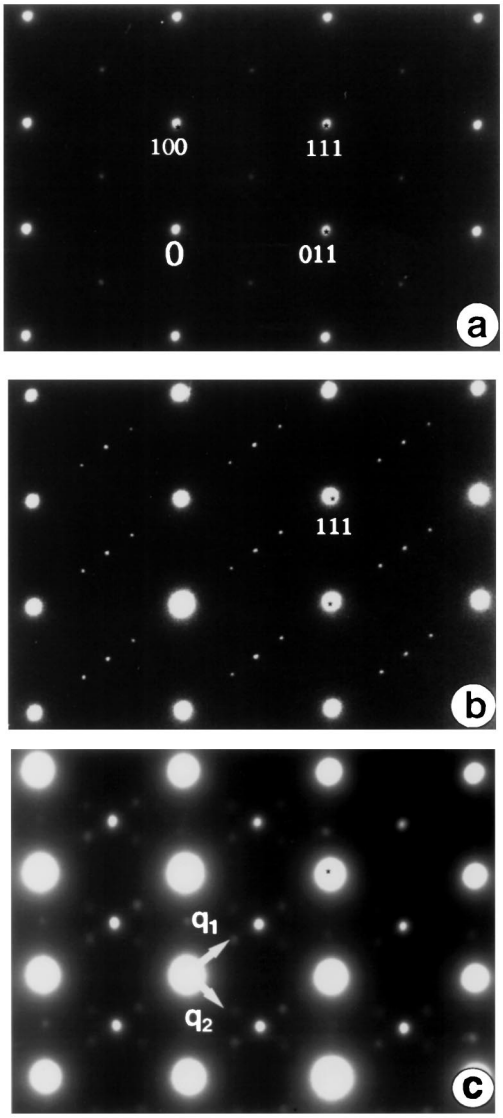

FIG. 3. $[01\bar{1}]$ zone-axis electron diffraction pattern of $La_{0.3}Sr_{0.7}FeO_3$ obtained at (a) room temperature and (b) 110 K (the presence of superlattice reflections along the $\langle 111 \rangle$ direction is evident), and (c) electron diffraction pattern exhibiting the presence of twin domains.

superstructural spots have been observed in the sample with nominal composition of $La_{0.3}Sr_{0.7}FeO_3$ ($x = 0.7$), which was investigated most thoroughly in past studies [6–8]. In Figs. 3(a) and 3(b), we show the $[01\bar{1}]$ zone-axis electron diffraction patterns obtained at room temperature and 110 K, respectively. Here we also adopt the simple cubic perovskite notion as that in previous studies. The most striking feature revealed in Fig. 3(b) is that a series of sharp superstructural reflections appears along the $\langle 111 \rangle_{\mathbf{p}}$ direction in addition to the basic Bragg diffraction spots. These superstructure spots become visible below ~200 K. Because of the heating effect and dynamical nature of the electron scattering, a precise measurement of the transition temperature is difficult in the present case. In fact, the superstructural spots can be also found along the other crystallographically related directions. Two sets of superstructural reflections around each basic Bragg spot are commonly observed, and which likely originate from different areas where the superstructural variants are related by twinning. A typical electron diffraction pattern is presented in Fig. 3(c), in which two sets of superstructural reflections are indicated as q_1 and q_2. By cooling and heating between room temperature and 110 K, the temperature dependence of this superstructure has been investigated. Normally, the weak satellite reflections become visible just below 200 K, then the intensities increase rapidly with the decrease of temperature. Anyway, no significant change of the periodicity of the modulation has been observed in our experiments.

The detection of superlattice spots at low temperatures provides the direct structural evidence of CO as suggested to occur at ~207 K from previous measurements (e.g., transport, magnetic susceptibility, Mössbauer spectrum, and neutron diffraction) [6–9]. In $La_{0.33}Sr_{0.67}FeO_3$, it was postulated [6] that the ordering of Fe^{3+} and Fe^{5+} ions occurs over crystallographically distinct sites in the ordered sequence of ...335335... along the $\langle 111 \rangle_{\mathbf{p}}$ direction of perovskite structure. The neutron magnetic scattering also revealed that the ordered state of magnetic moments includes the ferromagnetic Fe^{3+}-Fe^{5+} superexchange in addition to antiferromagnetic Fe^{3+}-Fe^{3+}

coupling, showing the spin density modulation with the wave vector of $a_p^*(\frac{1}{6}, \frac{1}{6}, \frac{1}{6})$. Such a CO transition should generate a periodic structural modulation involving atomic displacements with the wave vector of $a_p^*(\frac{1}{3}, \frac{1}{3}, \frac{1}{3})$. This is well consistent with the results we obtained. Electrons diffraction at large angle, of course, do not scatter directly from charge density; instead, they are diffracted by the atomic displacements induced by CO. Considering the large intensity of the satellite spots at 110 K, it can be concluded that the local structure would deviate significantly from the average structure. It seems to reasonable to expect that Fe^{5+} cations will occupy smaller octahedral sites than Fe^{3+} cations due to the coupling with the breathing-type distortions of FeO_6 octahedra. Consequently, a periodic structural modulation would be induced along the $\langle 111 \rangle_{\mathbf{p}}$ direction. Our investigation also indicated that same charge ordered state (structural modulation) exists over the range of composition $0.5 \leq x \leq 0.7$. So it seems that further explanations of the charge disproportionation as well as structural transformation in this system would be related to the fact that the charge states may be nonintegral [6,11].

Figure 4 shows a structural model for the antiferromagnetic CO state in $La_{1-x}Sr_xFeO_3$ ($x = \frac{2}{3}$), which is based on the magnetic neutron scattering measurement [6] as well as the present structural study. It is likely that the t_{2g} electrons are localized forming the local spin ($S = \frac{3}{2}$) and the e_g electrons, whose spins are coupled with t_{2g} spin via Hund's rule coupling, may change a character from itinerant to localized upon the CO transition. By analyzing the Mössbauer parameters for a selection of relevant compounds containing iron in 6-coordination [6], the magnetic moments and actual charges have been expected to be around $4.1\mu_B$ and $+3.2$ for nominal "Fe^{3+}" ions and $2.1\mu_B$ and $+4.2$ for nominal "Fe^{5+}." The issue of magnetic ordering in response to the CO in transition oxides has been studied theoretically in several papers [12]. The holes were found to condense onto the magnetic domain walls. In the present case, we expect that the maximum of the hole density modulation coincides with a minimum of spin density wave, as illustrated in Fig. 4. The phase of the spin modulation on Fe ions with respect to the lattice has been selected arbitrarily. The hole density has been drawn with some artistic license on Fe positions.

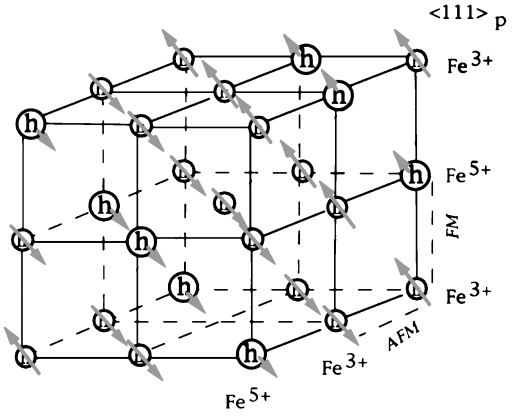

FIG. 4. Structural model exhibiting the spin density modulation (on Fe ions, indicated by arrows) and hole density modulation (indicated by circles) with respect to peroviskite structure.

In conclusion, a transmission electron microscopy study has revealed the exceedingly rich nature of structural modulations related to the charge ordering in the $La_{1-x}Sr_xFeO_3$ ($0 \leq x \leq 0.7$) system. It has been shown that there are different kinds of CO states at the low and high Sr-doping levels, respectively. The transformation of charge ordered states may be related to the change in the nominal hole concentration x as well as structural modification induced by Sr doping. According to the high resolution electron micrographs obtained at low temperatures, we have proposed a novel charge segregation phenomenon occurring in $La_{0.7}Sr_{0.3}FeO_3$. In $La_{0.3}Sr_{0.7}FeO_3$ ($x = 0.7$), the presence of structural modulation related to CO in the sequence $\ldots Fe^{3+}Fe^{3+}Fe^{5+}Fe^{3+}Fe^{3+}Fe^{5+}\ldots$ along the $\langle 111 \rangle_{\mathbf{p}}$ axis direction has been directly identified.

The authors express thanks to Mr. C. Tsuruta for his assistance. The work reported here was in part supported by the COE project organized by the Science and Technology Agency, and by a Grant-In-Aid for Scientific Research from the Ministry of Education, Japan.

*Permanent address: National Laboratory for Superconductivity, Institute of Physics, Chinese Academy of Sciences, Beijing, China.

[1] J. G. Bednorz and K. A. Müller, Z. Phys. B **64**, 189 (1986).
[2] V. J. Emergy, S. A. Kivelson, and H. Q. Lin, Phys. Rev. Lett. **64**, 475 (1990).
[3] Y. Tomioka, A. Asamisu, Y. Moritomo, H. Kuwahara, and Y. Tokura, Phys. Rev. Lett. **74**, 5108 (1995); C. H. Chen *et al.*, Phys. Rev. Lett. **76**, 4042 (1996); S. M. Hayden *et al.*, Phys. Rev. Lett. **68**, 1061 (1992).
[4] K. Chabara, T. Ohno, M. Kasai, and Y. Kozono, Appl. Phys. Lett. **63**, 1990 (1993).
[5] R. von Helmolt, J. Weckerg, B. Holzapfel, L. Schultz, and K. Samwer, Phys. Rev. Lett. **71**, 2331 (1993); Y. Tokura *et al.*, J. Phys. Soc. Jpn. **63**, 3931 (1994).
[6] P. D. Battle, T. C. Gibb, and P. Lightfoot, J. Solid State Chem. **84**, 271 (1990).
[7] M. Takano and Y. Takeda, Bull. Inst. Chem. Res. Kyoto Univ. **61**, 406 (1983).
[8] S. K. Park, S. Yamaguchi, and Y. Tokura (unpublished); J. Q. Li *et al.* (to be published).
[9] U. Shimoney and J. M. Kundsen, Phys. Rev. **144**, 361 (1966); P. K. Gallagher and J. B. MacChesney, Symp. Faraday Soc. **1**, 40 (1968).
[10] S.-W. Cheong, H. Y. Hwang, C. H. Chen, B. Batlogg, L. W. Rupp, Jr., and S. A. Carter, Phys. Rev. B **49**, 7088 (1994).
[11] M. Takano, J. Kawachi, N. Nakanishi, and Y. Takeda, J. Solid State Chem. **39**, 75 (1981).
[12] D. Poilblanc and T. M. Rice, Phys. Rev. B **39**, 9749 (1989); J. Zaanen and O. Gunnarsson, Phys. Rev. B **40**, 7391 (Rev. Lett. **64**, 1445 (1990).